Interstellar Silicon−Nitrogen Chemistry. 4. Which Reaction Paths to HSiN and HNSi? An Extensive *ab Initio* Investigation with Crucial Consequences for Molecular Astrophysics

O. Parisel,*,† M. Hanus, and Y. Ellinger

Laboratoire de Radioastronomie Millimétrique—URA 336, Equipe d'Astrochimie Quantique, Observatoire de Paris et Ecole Normale Supérieure, 24, rue Lhomond, F. 75231 Paris Cedex 05, France

Received: June 27, 1996; In Final Form: October 4, 1996[⊗]

In order to provide a possible explanation for the lack of detection of both HSiN and HNSi in the interstellar medium, an *ab initio* study of the $Si^+ + NH_3$ reaction is presented: it includes accurate energetic considerations and sketches dynamics discussions as well. It is unambiguously concluded that the X^1A_1 ground state of the $SiNH_2^+$ cation is the only exit channel of this reaction assuming interstellar conditions. The rotational and vibrational constants of this species are reported to stimulate its experimental and astrophysical searches. Upon dissociative recombination, it is likely that $SiNH_2^+$ can evolve toward HNSi: unfortunately, the dramatic weakness of the dipole moment of the latter species (0.05 D) makes it an unlikely candidate for today's radiotelescopes. At variance with HNSi, the high dipole moment value of HSiN (4.5 D) would make it a much more attractive candidate for astrophysical searches, but under interstellar conditions, we show that it can derive neither from the unimolecular HNSi ↔ HSiN equilibration nor from the $Si^+ + NH_3$, $N + SiH_3^+$ or $N^+ + SiH_3$ reactions as sometimes incorrectly stated in the astrophysical models that deduce interstellar silicon chemistry from that of carbon. Throughout this study, the very hazardous character of conclusions deduced from isoelectronic considerations should be considered as the leading feature: the finishing stroke to such isoelectronic analogies is given by our study of the $H^+ + HNSi \leftrightarrow HSiN + H^+$ reactions which leads to the conclusion that HSiN might be unlikely to survive interstellar hydrogenation processes.

1. Introduction

Until recently, interstellar silicate species were supposed to be embedded in grains,[1] but the detection of the free SiN radical in space[2,3] has drawn attention to the gas phase chemistry of azasilicated molecules.[4,5] Searches for the related HNSi and HSiN triatomics have been undertaken, but neither of them has been identified in the interstellar medium (ISM) to the present day.

When compared with carbon chemistry, this situation appears rather puzzling. Following the pioneering identification of the CN radical,[6] both HCN and its low-lying HNC isomer were observed in the ISM (see ref 7 and references therein), as, more recently,[8,9] has been the linear $HCNH^+$ species.

1.1. From the HCN/HNC Chemistry.... As a consequence of astrophysical observations, the following reaction scheme has been hypothesized to explain the formation of CN, HCN, HNC, and $HCNH^+$, as well as the value of the HCN/HNC ratio in model clouds:[7,10]

$$C^+(X^2P) + NH_3(X^1A_1) \rightarrow HCNH^+ + H \quad (1)$$

$$HCNH^+ + e^- \rightarrow HCN + H \quad (2)$$

$$HCNH^+ + e^- \rightarrow HNC + H \quad (3)$$

$$HCN + h\nu \rightarrow H + CN \quad (4)$$

$$HNC + h\nu \rightarrow H + CN \quad (5)$$

This series of reactions has been the subject of many studies and has now stood the tests of laboratory experiments and quantum chemistry investigations.[11,12] It is now well established that reaction 1 proceeds through the formation of the long-range CNH_3^+ (C_{3v} X^2E) precursor which further undergoes a series of transformations, with no activation barrier, to the linear $HCNH^+$ ($C_{\infty v}$ $X^1\Sigma^+$) cation. Upon dissociative recombination (reactions 2 and 3), both HCN and HNC are then produced: they furthermore can photodissociate to CN (reactions 4 and 5). Although reactions 4 and 5 are likely to occur in diffuse clouds and in the external envelopes of dark and dense clouds as well, HCN and HNC are more likely to be destroyed in dark clouds by dominant ions, *e.g.* H_3^+, He^+, C^+, and HCO^+.

1.2. ... To that of the HSiN/HNSi System? Only a few experimental data are usable and even available when turning from the carbon− to the silicon−nitrogen chemistry. HNSi was first detected thanks to the pioneering matrix experiments by Ogilvie and Cradock.[13] More recently, Maier and Glatthaar[14] succeeded in recording the infrared (IR) spectra of both HSiN and HNSi trapped in argon matrices.[15] Gas phase rotational spectra of HNSi have been obtained by several groups;[16,17] all of them failed, however, to produce HSiN in analogous conditions, whatever the precursors were. One possible explanation for the difficulties encountered in producing HSiN may be that it lies 55 kcal/mol above the lower HNSi isomer (Table 1). If one remembers, however, that the interstellar HCN/HNC ratio is not governed by thermodynamic equilibria, one might *a priori* expect that the detection of the lowest HNSi species could stimulate the search for its higher HSiN isomer even if ΔE(HSiN/HNSi) ≫ ΔE(HNC/HCN).Two different schemes can be investigated when seeking for reaction paths leading to HSiN and HNSi.

First of all, the formation of one of the two isomers followed by its transformation into the other can be considered. However, as shown in Table 1, the barriers to the isomerization are higher than 40 kcal/mol for HSiN → HNSi and 100 kcal/mol for the HSiN ← HNSi reversed reaction. Such unimolecular processes are thus highly improbable in ISM conditions owing to the lack of any available external energy. Two possibilities remain,

† E-mail: parisel@vega.ens.fr.

⊗ Abstract published in *Advance ACS Abstracts,* November 15, 1996.

S1089-5639(96)01844-0 CCC: $14.00

TABLE 1: Energetics (kcal/mol), Geometries (Å and deg), and Rotational Constants for the HNSi/HSiN System with the 6-311++G Basis Set**

	MP2	MP4
HSiN ($X^1\Sigma^+$)		
r_{SiN}	1.622	1.667
r_{SiH}	1.478	1.496
μ (D)[a]	4.50	
B_0 (GHz)[a]	18.734	
HNSi ($X^1\Sigma^+$)		
r_{SiN}	1.569	1.577
r_{NH}	1.006	1.007
μ (D)[a]	0.05	
B_0 (GHz)[a]	19.019	
(N···H···Si)†		
r_{SiN}	1.573	1.587
r_{SiH}	1.496	1.504
∠HSiN	89.8	88.3
ΔE(HNSi−HSiN)	59.7	55.0
E_{Act} (HNSi → HSiN)	101.0	89.2
E_{Act} (HNSi ← HSiN)	41.3	34.2

[a] Best estimate from ref 18.

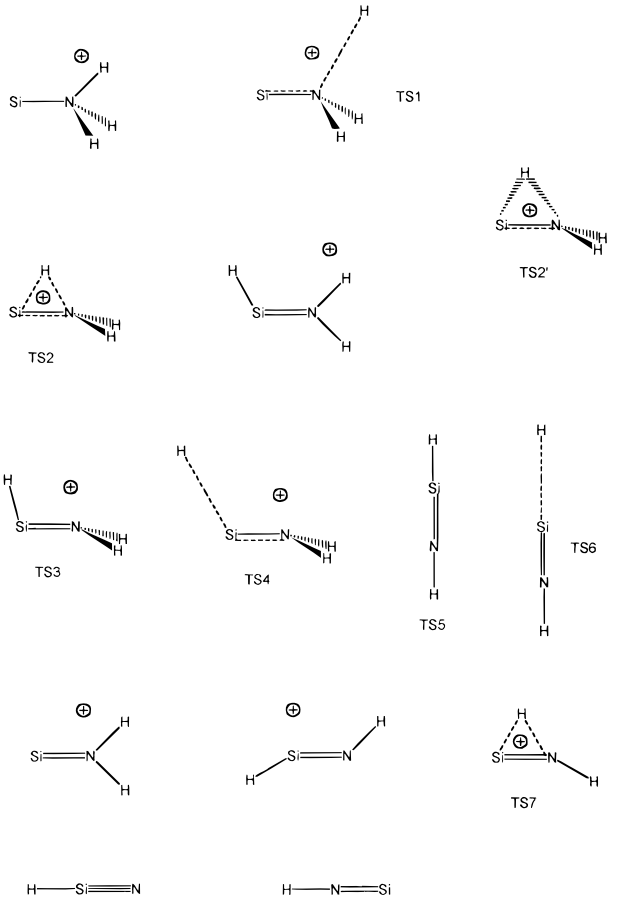

Figure 1. Structures of the stationary intermediates along the $Si^+ + NH_3$ potential energy surface.

however: either having the barriers crossed through tunneling or considering a bimolecular reaction to ensure the HSiN ↔ HNSi interconversion. The former point will not be discussed further here whereas it is worth noting that coupling reactions 1−5 to

$$HCN + H \leftrightarrow CNH + H \quad (6)$$

explains, at least partly, the observed variations of the HCN/HNC ratio relative to interstellar kinetic temperature fluctuations.[19,20] An analogous reaction may be essential in the discussion of the relative abundances of HNSi and HSiN in molecular clouds, as will be discussed in section 7.

The second scheme relies on crude valence isoelectronic considerations between Si and C to derive reactions expected to simultaneously lead to both HSiN and HNSi.[4] Three of them have been proposed:

$$N + SiH_3^+ \rightarrow \text{products} \quad (7)$$

$$N^+ + SiH_3 \rightarrow \text{products} \quad (8)$$

$$Si^+ + NH_3 \rightarrow \text{products} \quad (9)$$

Reactions 7 and 8, assuming they are energetically allowed in interstellar conditions, suffer the drawback that the molecular abundances of N^+, SiH_3^+, and SiH_3 may not be high enough to ensure a noticeable formation of products. They will, however, be detailed in section 5 since they might be of interest to analyze laboratory experiments. Reaction 9 derives from a straightforward analogy with the carbon−nitrogen chemistry. According to such an assumption, Si^+ reacts on NH_3: this finally results in atomic hydrogen and in an (H, H, Si, N)$^+$ complex that undergoes further dissociative recombinations to HSiN or HNSi. Such an approach, however, makes the implicit hypothesis that the intermediate possesses a H−Si−N−H connectivity, as proved for the (H, H, C, N)$^+$ system.

The aim of the present report is to comprehensively assess whether the analogy made with the carbon chemistry is relevant or not when dealing with silicon. Such a scope necessarily requires a quantitative study of the $Si^+ + NH_3$ reaction with special emphasis on exit channels within the (H, H, Si, N)$^+$ manifold (section 3) as well as the accurate determination of possible energy barriers along the paths leading to the products (section 4). Some dynamical aspects of this reaction are sketched in section 4.5. Finally, section 7 investigates the propensity for HSiN to survive interstellar conditions.

2. Methodologies and Computational Details

The calculations have been performed at increasing levels of theory: MP2, MP3, MP4, CCSD(T), and even full-valence CASSCF (complete active space self-consistent field), FOCI (first-order configuration interaction), and SOCI (second-order configuration interaction) when necessary. The definition of the CAS-CI, FOCI, and SOCI variational spaces is given in refs 18, 21, and 22 (hereafter referred to as parts I−III in this series of papers) as is the procedure used to obtain excited states from the MC/P methodology, which couples variational and multireference perturbation treatments to ensure that nondynamical and dynamical correlation effects are accurately described.[23,24]

A large flexibility of the one-particle space (approaching the so-called Hartree−Fock limit) is reached by using a triple-zeta basis set, extended by polarization and diffuse functions[25,26] on each atom. Exponents and contraction coefficients are those of the 6-311++G** basis set[27] for hydrogen and nitrogen while the augmented triple zeta contraction by McLean and Chandler[28] is retained for silicon under the previous acronym.

In the MPn and CCSD(T) calculations, all electrons are correlated. *All* geometries are fully optimized, with the exception that CCSD(T) calculations use the fully-optimized MP4 geometries. The GAUSSIAN-92 code has been used for the MP2, MP4, and CCSD(T) calculations.[29]

When indicated, absolute energies have been corrected for zero-point vibrational energy (ZPE): these corrections are made using carefully scaled vibrational wavenumbers. Although it would have been possible to determine the ZPE corrections at the MP4 and CCSD(T) levels of calculation, it has been found

wiser in the present context to use the scaled MP2 correction as such for these methods. The MP2 scaling factor needed in this report has been deduced from a calibration study[18] on the experimental IR spectra of HNSi, HSiN, H_2SiNH and $HSiNH_2$: it amounts to 0.959 and has been applied to wavenumbers.

In order to account for possible artifacts originating from the variation of the one-particle space when going from isolated species to chemically interacting ones along reaction paths (the so-called basis set superposition error, BSSE), energies were also corrected, when indicated, using the counterpoise technique by Boys and Bernardi:[30,31] if two fragments A and B, with respective geometries and atomic basis sets ($\mathbf{r}_A$,{χ_A}) and ($\mathbf{r}_B$,{χ_B}), interact and lead to a *long-range* complex (AB), the BSSE-corrected stabilization energy ΔE_{corr} is given by

$$\Delta E_{corr} = \Delta E_{uncorr} + \epsilon_{BSSE}$$

where

$$\Delta E_{uncorr} = E_{AB}(\mathbf{r}_{AB},\{\chi_A\} \cup \{\chi_B\}) - E_A(\mathbf{r}_A,\{\chi_A\}) - E_B(\mathbf{r}_B,\{\chi_B\})$$

and

$$\epsilon_{BSSE} = E_A(\mathbf{r}_{AB},\{\chi_A\}) + E_B(\mathbf{r}_{AB},\{\chi_B\}) - E_A(\mathbf{r}_{AB},\{\chi_A\} \cup \{\chi_B\}) - E_B(\mathbf{r}_{AB},\{\chi_A\} \cup \{\chi_B\})$$

These quantities were determined for the MP2 and MP4 reaction paths and the MP4 corrections were applied as such to the CCSD(T) energies.

When describing molecular or atomic configurations, *KK* is used to indicate a set of closed shells that are not involved in the investigated chemical process. In any figure, *points* and *crosses* respectively stand for *in-plane* and *out-of-plane* electrons. It is worth noting that $2s_N$ or $3s_{Si}$ electrons are not pictured when dealing with atomic systems, at variance with molecular species.

3. The (Si, N, H, H)$^+$ Potential Energy Surface

The study of any reaction requires the investigation of possible exit channels. In particular, when dealing with gas phase astrochemistry, it is primordial to focus on those that are either exothermic or athermic. A careful investigation of the (Si, N, H, H)$^+$ potential energy surface has thus been performed using the methodologies quoted in section 2. The results have been detailed elsewhere (parts I−III in this series), so that only the conclusions necessary to the understanding of the present work are developed here. Preliminary studies of this surface have been reported earlier;[32−36] it is strongly believed, however, that the methodologies used were not accurate enough to derive unquestionable conclusions.

First of all, our results unambiguously confirm that the absolute minimum of the (Si, N, H, H)$^+$ potential energy surface is the X^1A_1 ground state of the C_{2v} species $SiNH_2^+$ (Table 2). To our knowledge, there is no direct spectroscopic evidence of this fact: only indirect conclusions have been deduced from experimental data. For example, the elusive existence of $SiNH_2^+$ has been proposed to rationalize recent gas phase "collisional activation" and "neutralization−reionization" mass spectroscopy experiments;[37,38] no related species with SiH connectivity was simultaneously detected, starting from a mixture of iodosilane and ammonia, or of iodosilane and dinitrogen. Previously, Wlodek et al.[39] had reported the formation of $SiNH_2^+$ in experiments dedicated to the determination of the proton affinity of HNSi; the interesting species was produced according to reaction 9 at $T = 295$ K and $P = 0.35$ Torr. Such experimental conditions may not be too relevant for this reaction in interstellar conditions. In order to stimulate further observational and spectroscopic investigations, the computed rotational constants of $SiNH_2^+$ (X^1A_1) have been gathered in Table 3. Taking the center of mass of the cation as the origin, our best estimate of the dipole moment is 0.5 D at the most reliable SOCI level of calculation;[21] although weak, it might be enough for a radiodetection in space, provided the abundance of this ion is high enough. Accurate geometries are given in Tables 4 and 5, scaled IR wavenumbers are collected in Table 6. The electronic absorption spectrum of this species, which will be required in some forthcoming sections, and a further analysis of the spectral signatures have been discussed in part II of this series.

TABLE 2: Relative Energies (kcal/mol) for the (H, H, Si, N)$^+$ System[a]

compd	state	MP2	MP4
$SiNH_2^+$	X^1A_1	0.00	0.00
H_2SiN^+	X^3A_2	123.7	119.0
$HSiNH^+$	X^1A'	52.2	52.3
$HSiNH^+$	a^3A'	97.5	96.7
$SiNH_2^+$	1^3B_2	84.8[b]	
H_2SiN^+	1^3B_2	131.8[b]	

[a] The 6-311++G** basis set is used. All geometries are fully optimized except those of the excited 1^3B_2 states that correspond to the fully-optimized (MP4) geometry of the corresponding ground state. [b] *Lowest* excited vertical state (see refs 21 and 22).

TABLE 3: Recommended Rotational Constants for $SiNH_2^+$ and for Some Isotopomers (GHz)

isotopomer	A_0	B_0	C_0
$^{28}Si^{14}NH_2^+$	357.418	16.263	15.555
$^{28}Si^{14}NHD^+$	246.877	15.009	13.865
$^{28}Si^{14}ND_2^+$	178.709	14.020	12.739
$^{29}Si^{14}NH_2^+$	357.418	16.063	15.066
$^{30}Si^{14}NH_2^+$	357.418	15.877	14.898
$^{28}Si^{15}NH_2^+$	357.418	15.742	14.778

As seen from Table 2, the lowest-lying compound having the H−Si−N−H connectivity is the floppy singlet ground state of $HSiNH^+$ that is found to lie 52 kcal/mol above $SiNH_2^+$ (X^1A_1); 45 kcal/mol higher comes the *cis*-bent a^3A' state of $HSiNH^+$. An accurate study of both these species is given in part I of this series. Finally, the silicahydrogenated counterpart of $SiNH_2^+$, namely H_2SiN^+ (C_{2v} X^3A_2), lies 120 kcal/mol above the minimum of the potential energy surface (part III of this series). Those stationary points on the (H, H, Si, N)$^+$ surface that correspond to bimolecular systems all lie more than 100 kcal/mol above the $SiNH_2^+$ ground state.[37]

It follows that the isomers' ordering is different if considering the (Si, N, H, H)$^+$ system (Table 2) or the (C, N, H, H)$^+$ system (Table 7): *a different chemistry must be expected when exchanging carbon for silicon*.

4. The $Si^+ + NH_3$ Reaction

4.1. Thermodynamics Aspects. Let us now turn toward the search for the athermic or exothermic exit channels, triplet or singlet, of the $Si^+ + NH_3$ reaction. As seen from the energetics reported in Tables 8 and 9, only the channel leading to $SiNH_2^+(X^1A_1)$ corresponds to an exothermic reaction if the reactants are taken in their ground states, which is the common

TABLE 4: Optimized Geometries (MP2/6-311++G) of Stationary Points along the $Si^+ + NH_3$ Reaction Paths (Angles in deg, Bond Lengths in Å)**

	$Si^+ + NH_3$ C_{3v}	$SiNH_3^+$ C_{3v}	$SiNH_2H_a^+$ C_s TS_1	TS_2 C_s	TS_2' C_1	$HSiNH_2^+$ planar	$HSiNH_2^+$ C_s TS_3	$HSiNH_2^+$ C_s TS_4	$H + SiNH_2^+$ C_{2v}
d(SiN)	∞	2.020	1.701	1.785	1.786	1.652	1.671	1.663	1.662
d(NH_1)	1.014	1.026	1.025	1.028	1.022	1.017	1.019	1.022	1.022
d(NH_2)	1.014	1.026	1.025	1.023	1.022	1.017	1.019	1.022	1.022
d(NH_3)	1.014	1.024	1.584		1.451				∞
d(SiH_3)				1.655	1.656	1.475	1.493	2.402	
∠$SiNH_1$		114.71	118.67	125.33	123.7	124.17	122.43	123.55	124.83
∠$SiNH_2$		114.71	118.67	123.72	121.2	123.34	122.43	123.55	124.83
∠$SiNH_3$		111.58	124.24						
∠$NSiH_3$				49.67	49.5	117.31	116.42	99.18	
α	111.6	121.51	112.95		25.0[a]				
A (diedral $H_{1,2}$)							104.04	103.0	

[a] Out-of-plane angle relative to the initial molecular plane of TS_2.

TABLE 5: Optimized Geometries (MP4/6-311++G) of Stationary Points along the $Si^+ + NH_3$ Reaction Paths (Angles in deg; Bond Lengths in Å)**

	$Si^+ + NH_3$ C_{3v}	$SiNH_3^+$ C_{3v}	$SiNH_2H_a^+$ C_s TS_1	TS_2 C_s	$HSiNH_2^+$ planar	$HSiNH_2^+$ C_s TS_3	$HSiNH_2^+$ C_s TS_4	$H + SiNH_2^+$ C_{2v}
d(SiN)	∞	2.026	1.707	1.807	1.655	1.683	1.667	1.662
d(NH_1)	1.019	1.026	1.025	1.028	1.020	1.021	1.023	1.022
d(NH_2)	1.019	1.026	1.025	1.024	1.017	1.021	1.023	1.022
d(NH_3)	1.019	1.024	1.612					∞
d(SiH_3)				1.657	1.480	1.501	2.443	
∠$SiNH_1$		111.54	119.24	125.50	123.27	122.31	123.54	124.86
∠$SiNH_2$		111.54	119.24	123.74	124.07	122.31	123.54	124.86
∠$SiNH_3$		114.68	123.15					
∠$NSiH_3$				49.08	116.53	114.70	98.15	
α	107.0	121.50	111.79					
A (diedral $H_{1,2}$)						104.0	103.0	

TABLE 6: Scaled[a] MP2/6-311++G Wavenumbers (cm^{-1}) for Stationary Points along the $Si^+ + NH_3$ Reaction Paths**

NH_3 C_{3v}	$SiNH_3^+$ C_{3v}	$SiNH_2H_a^+$ C_s TS_1	TS_2 C_s	TS2′ C_1	$HSiNH_2^+$ planar	$HSiNH_2^+$ C_s TS_3	$HSiNH_2^+$ C_s TS_4	$SiNH_2^+$ C_{2v}
1026 A_1	279i A″	2977i A′	1480i A′	1466i A	552 A″	888i A″	476i A′	556 B_2
1597 E	426 A′	577 A″	595 A″	595 A	592 A′	465 A′	141 A″	629 B_1
3385 A_1	699 A′	597 A′	668 A″	673 A	661 A″	636 A″	200 A′	939 A_1
3530 E	1355 A′	838 A″	795 A′	768 A	864 A′	660 A′	544 A″	1482 A_1
	1418 A″	869 A′	917 A′	864 A	976 A′	905 A′	633 A′	3343 A_1
	1547 A′	1009 A′	1500 A′	1467 A	1517 A′	1485 A′	930 A′	3427 A_1
	3283 A′	1481 A′	1627 A′	1601 A	2199 A′	2068 A′	1481 A′	
	3356 A″	3315 A′	3279 A′	3276 A	3387 A′	3374 A′	3345 A′	
	3397 A′	3385 A″	3393 A″	3369 A	3485 A″	3459 A″	3421 A″	

[a] The *ab initio* values have been scaled as described in section 2.

TABLE 7: Relative Energies (kcal/mol) for the $(H, H, C, N)^+$ System[40]

	state	energy
lin-$HCNH^+$	$X^1\Sigma^+$	0.00
H_2NC^+	X^1A_1	42.0
H_2NC^+	a^3B_2	97.2
H_2CN+	X^3B_2	104.7
cis-$HCNH^+$	$^3A'$	105.3
trans-$HCNH^+$	$^3A'$	113.6

assumption when dealing with astrochemistry in dark and dense interstellar clouds. As an important consequence for astrophysics, it follows that *only* $SiNH_2^+(X^1A_1)$ may be formed from Si^+ and NH_3; a further dissociative recombination of this species leading to HNSi appears then relevant. At variance, HSiN is unlikely to be produced following the same mechanism. Whether the formation of $SiNH_2^+(X^1A_1)$ proceeds with an activation barrier or not from $Si^+ + NH_3$ is discussed in the next subsections. In the following, it must be kept in mind that the excited states quoted in Table 2 are the *lowest* ones for a given connectivity; any other excited state that may be involved in section 4.3 and in section 4.4 lies above them.

4.2. The $SiNH_3^+$ Long-Range Complex. The three-fold spatial degeneracy of the X^2P ground state of Si^+ is removed when the symmetry is lowered from R_3 to C_{3v} upon complexation with $NH_3(X^1A_1)$. This results in three electronic states of the $SiNH_3^+$ entity:

$$KK \,||\, \sigma_{SiN}^2\, 3p_{Si,-1}^1\, \alpha_{SiN}^{*0} \tag{10}$$

$$KK \,||\, \sigma_{SiN}^2\, 3p_{Si,+1}^1\, \alpha_{SiN}^{*0} \tag{11}$$

$$KK \,||\, \sigma_{SiN}^2\, 3p_{Si,\pm1}^0\, \alpha_{SiN}^{*1} \tag{12}$$

Configurations 10 and 11 are degenerate and form a X^2E state, while configuration 12 leads to a $^2A_1$ state: it is certainly repulsive and is thus of no interest here. A further symmetry-lowering to C_s splits the ^2E state into its $^2A'$ and $^2A''$ components whereas the upper $^2A_1$ state correlates to $^2A'$ (Figure 2).

As seen from Tables 4, 5, and 8 and as illustrated by a deep well in Figure 3, the first step of reaction 9 consists in the formation of the long-range complex $SiNH_3^+$ ($r_{SiN} = 2.02$ Å). Inspection of Table 6 reveals the existence of one imaginary frequency for this species. Actually, the C_s symmetry has been retained instead of C_{3v} symmetry, so that only one component of the X^2E state ($^2A'$ or $^2A''$) has been handled in the

TABLE 8: Energetics of the $Si^+ + NH_3$ Reaction (Energies Are in atomic units; 6-311++G Basis Set Used)**

	$Si^+ + NH_3$ C_{3v}	$SiNH_3^+$ C_{3v}	$SiNH_2H_a^+$ C_s TS_1	TS_2[e] C_s	$HSiNH_2^+$ planar	$HSiNH_2^+$ C_s TS_3	$HSiNH_2^+$ C_s TS_4	$H + SiNH_2^+$ C_{2v}
MP2								
initial	−345.021 443	−345.112 203	−345.016 338	−345.031 515	−345.110 754	−345.083 099	−345.045 818	−345.049 228
BSSE		+0.005 662	−0.000 823				−0.001 430	
ZPE[a]	+0.033 410	+0.035 267	+0.027 500	+0.029 016	+0.032 477	+0.029 728	+0.024 364	+0.023 639
total	−344.988 033	−345.071 274	−344.989 661	−345.002 499	−345.078 277	−345.053 371	−345.022 884	−345.025 589
MP4								
initial	−345.199 096	−345.290 673	−345.196 613	−345.214 577	−345.284 027	−345.257 390	−345.221 152	−345.224 189
BSSE		+0.006 763	−0.000 625				−0.001 352	
ZPE[b]	+0.033 410	+0.035 267	+0.027 500	+0.029 016	+0.032 477	+0.029 728	+0.024 364	+0.023 639
total	−345.165 686	−345.248 643	−345.169 738	−345.185 561	−345.251 550	−345.227 662	−345.198 140	−345.200 550
CCSD(T)[c]								
initial	−345.201 051	−345.293 023	−345.196 613	−345.220 165	−345.285 838	−345.260 004	−345.223 804	−345.225 416
BSSE[d]		+0.006 763	−0.000 625				−0.001 352	
ZPE[b]	+0.033 410	+0.035 267	+0.027 500	+0.029 016	+0.032 477	+0.029 728	+0.0243 64	+0.023 639
total	−345.167 641	−345.250 993	−345.177 116	−345.191 149	−345.253 361	−345.230 276	−345.200 792	−345.201 777

[a] The *ab initio* values have been scaled as described in section 2. [b] The scaled MP2/6-311++G** values are used. [c] Single-point calculations using the MP4/6-311++G** fully optimized geometries. [d] The MP4/6-311++G** BSSE corrections are used. [e] The absolute energy for TS_2' is −345.033 566 au at the uncorrected MP2 level of calculations.

TABLE 9: Exothermicity (kcal/mol, Negative Values) or Endothermicity (Positive Values) for Different Exit Channels Starting from $Si^+ + NH_3$[a]

exit channel	state	MP2	MP4
$Si^+ + NH_3$	X^2P	0.00	0.00
$H + SiNH_2^+$	X^1A_1	−17.4	−15.7
$H + H_2 SiN^+$	X^3A_2	106.3	103.3
$H + HSiNH^+$	X^1A'	34.8	34.9
$H + HSiNH^+$	a^3A'	80.1	79.3
$H + SiNH_2^+$	1^3B_2	67.4	69.1
$H + H_2 SiN^+$	1^3B_2	114.4	116.1

[a] The 6-311++G** basis set is used. The X^2 S ground state of the neutral expelled hydrogen atom is assumed; NH_3 reacts in its X^1 A_1 ground state.

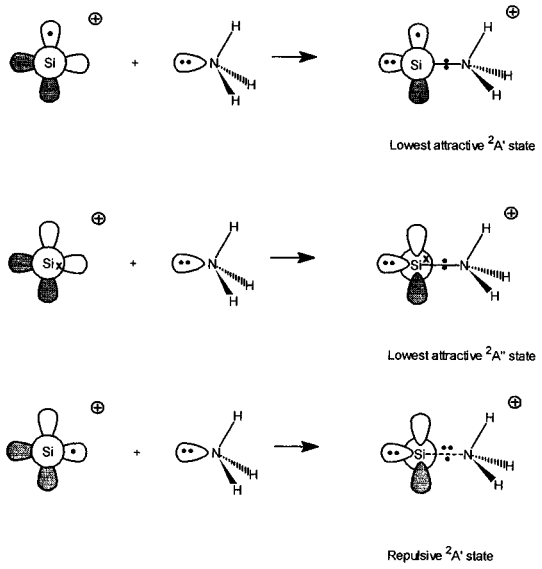

Figure 2. Formation of the long-range complex $SiNH_3^+$.

calculation: this might induce a slight artifact. It should, however, be kept in mind that such a ^2E state could be sensitive to a Jahn−Teller effect which intrinsically lowers the initial C_{3v} molecular symmetry to C_s or C_1. An accurate investigation of this secondary phenomenon is beyond the scope of this paper; preliminary investigations performed at the full-valence CASSCF level of theory show, however, that it is in fact negligible: both the $^2A'$ and $^2A''$ components remain degenerate within less than 1 kcal/mol. Whether a weak Jahn−Teller effect exists or not is nevertheless of limited importance for the present study; forthcoming conclusions will not be affected.

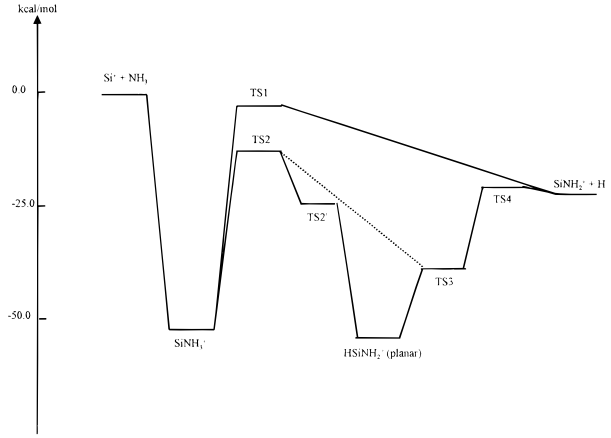

Figure 3. The (simplified) $Si^+ + NH_3$ potential energy surfaces.

As deduced from Table 8, the stabilization energy (kcal/mol) induced by the complexation process is estimated to 56.9 (MP2), 57.5 (MP4), and 57.7 (CCSD(T)). These values are reduced by about 1 kcal/mol when ZPE corrections are taken into account: 55.7 (MP2), 56.3 (MP4), and 56.5 (CCSD(T)). Finally, including the BSSE corrections, which are *positive* for the long-range $SiNH_3^+$ species, reduces the stabilization energy further: this is the common behavior in such cases. It is worth noting that the BSSE corrections are larger in magnitude than the ZPE corrections. The ultimate values, corrected for both BSSE and ZPE effects, turn out to be 52.1 (MP2), 52.1 (MP4), and 52.2 (CCSD(T)). Such an excess of energy is released into the vibrational modes of the complex.

4.3. Reaction Path A: One-Step Hydrogen Abstraction. *4.3.1. The $^2A'$ Potential Energy Surface.* From the $^2A'$ component in $SiNH_3^+(X^2E)$, a first reaction path (path A) is obtained through the in-plane stretch of a NH bond: this leads to the lengthened structure TS1 ($^2A'$ state) (Figure 1). As seen from Tables 4 and 5, the SiN bond length has been dramatically reduced relative to that of the initial precursor (1.71 vs 2.02 Å) and approximates that in $SiNH_2^+(X^1A_1)$. The $NH_{stretched}$ length, close to 1.59 Å, is far from the starting 1.025 Å value, while the other two remaining NH distances remain close to those of $SiNH_3^+$. As shown by the geometry analysis, TS1 thus appears as a transition state toward the dissociation to $H + SiNH_2^+$. This is confirmed by the vibrational analysis: the normal mode associated with the imaginary frequency (2977i cm^{-1}, A′ symmetry) corresponds to a NH stretch coupled with the motion of the remaining $(H, H, N, Si)^+$ skeleton toward a planar C_{2v}

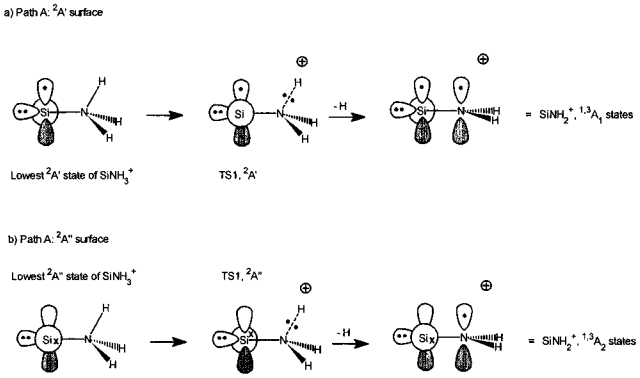

Figure 4. One-step hydrogen abstraction on $SiNH_3^+$ through TS1.

TABLE 10: BSSE- and ZPE-Corrected Reaction Barriers (ΔE_{act}, kcal/mol) for the $Si^+ + NH_3$ Reaction along Path A (Lowest^2 A′ Potential Energy Surface[a]

	MP2	MP4	CCSD(T)
electronic	+3.20	+1.56	−1.85
+ BSSE	+2.69	+1.17	−2.24
+ ZPE	−1.02	−2.54	−5.95

[a]The 6-311++G** basis set is used.

structure. Following the hydrogen abstraction diabatically, $SiNH_2^+$ is obtained with orbital occupancies as (Figure 4a):

$$KK \,||\, \sigma^2_{SiN}\, sp^2_{Si}\, 3p^0_{Si}\, p^1_{\pi,N}\, p^1_{\pi,Si} \qquad (13)$$

According to spin conservation along the doublet surface, the two unpaired electrons can couple either in a singlet state or in a triplet state, so that the previous configuration in fact adiabatically correlates to

$$KK \,||\, \sigma^2_{SiN}\, sp^2_{Si}\, \pi^2_{SiN}\, 3p^0_{Si} \qquad (14)$$

$$KK \,||\, \sigma^2_{SiN}\, sp^2_{Si}\, \pi^{\uparrow}_{SiN}\, \pi^{*\uparrow}_{SiN}\, 3p^0_{Si} \qquad (15)$$

Configuration 15 corresponds to the $\pi\pi^*$ excited 1^3A_1 state of $SiNH_2^+$ and leads to an endothermic reaction, whereas configuration 14 gives the X^1A_1 ground state of $SiNH_2^+$, in that case, the reaction is allowed in interstellar conditions according to the energetic considerations of Table 9 and section 4.1. The question whether this transition state induces a barrier or not for the $Si^+ + NH_3 \rightarrow SiNH_2^+(X^1A_1) + H$ process can be assessed from the absolute energies collected in Tables 8 and 10. At the MP2 and MP4 levels of calculation, small barriers (ΔE_{act}) of 3.20 and 1.56 kcal/mol are found. They are reduced by about 0.5 kcal/mol upon BSSE corrections; as seen in Table 8, the BSSE correction is *negative* for TS1, a structure that can be seen as the long-range complex (H)···($SiNH_2^+$). Finally, the inclusion of ZPE corrections dramatically reverses the sign of ΔE_{act}: the barrier disappears. Contrary to what has been pointed out in section 4.2, the ZPE correction is now larger than the BSSE correction and is sufficient to have the reaction proceed without thermodynamic barrier. At the CCSD(T) level of theory, no barrier is obtained, even if no correction is made.

Reaction Path A is thus allowed for the ^{2}A′ surface arising from the X^2E molecular state of the long-range complex; hence, the ground state of $SiNH_2^+$, the only reachable product according to simple thermodynamic considerations, can effectively be obtained under interstellar conditions.

4.3.2. The ^{2}A″ Potential Energy Surface. Starting from the second component of the X^2E state of $SiNH_3^+$ leads to the

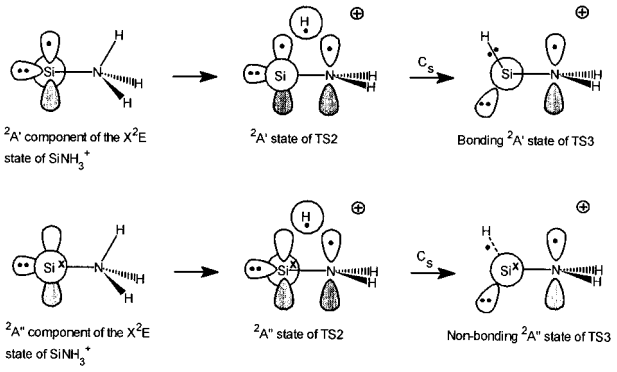

Figure 5. Formation of TS2 and TS3: the C_1 symmetry is retained along the reaction path.

^{2}A″ state of TS1. However, its dissociation would result in $SiNH_2^+$ with orbital occupancies:

$$KK \,||\, \sigma^2_{SiN}\, sp^2_{Si}\, 3p^1_{Si}\, \pi^1_{SiN} \qquad (16)$$

Remaining on a doublet potential energy surface for the products, configuration 16 adiabatically correlates to the lowest singlet state or to the lowest triplet states of $SiNH_2^+$ having an A_2 spatial symmetry (Figure 4b). The 1^1A_2 state lies 4.71 ev (108 kcal/mol) above the X^1A_1 ground state (part II of this series); the exit channel is highly endothermic (91 kcal/mol) and is thus closed in interstellar conditions even if no barrier is present along the related path. The same conclusion can be derived for the 1^3A_2 state since it lies 4.61 eV (106 kcal/mol) above the ground state of $SiNH_2^+$; in that case, the endothermicity becomes 89 kcal/mol.

4.4. Reaction Path B: Two-Step Hydrogen Abstraction. The previous reaction scheme proceeded directly through the rupture of a NH bond. Another possibility is to consider that the first step is the transfer of an hydrogen atom from nitrogen toward silicon, with retention of C_s symmetry, so that a SiH bond is formed. As seen in Figure 5, the ^{2}A′ component of the starting X^2E state of $SiNH_3^+$ leads to the final $HSiNH_2^+$−TS3 species with occupancies

$$KK \,||\, \sigma^2_{SiN}\, sp^2_{Si}\, 3p^0_{Si}\, \sigma^2_{SiH}\, p^1_{\pi,N} \qquad (17)$$

whereas those obtained considering the ^{2}A″ components would be

$$KK \,||\, \sigma^2_{SiN}\, sp^2_{Si}\, 3p^1_{Si}\, \sigma^1_{SiH}\, p^1_{\pi,N} \qquad (18)$$

If the molecular plane is retained, the ^{2}A′ potential energy surface ensures the existence of a SiH bond (σ^2_{SiH}) in the ^{2}A′ state of TS3 whereas the ^{2}A″ surface certainly does not: due to the single occupancy of the new σ_{SiH} orbital, the corresponding state of the resulting TS3 may be dissociative or at least lies too high in energy to be reachable. Upon such a rotation, a first transition state is obtained, TS2 (^{2}A′ state, Figure 1); it is characterized by the bridged location of the rotating hydrogen atom (Figure 5) and has one imaginary frequency (A′ symmetry, 1480i cm^{-1}) that strongly couples the rotation of the hydrogen atom around nitrogen and the stretch of the SiN bond. Relaxing any symmetry constraint on TS2 leads to the planar structure $HSiNH_2^+$ (Figure 6); its ^{2}A′ ground state lies slightly below (less than 2 kcal/mol according to Table 8) the C_{3v} structure of $SiNH_3^+(X^2E)$. Assuming a diabatic correlation from TS2 through the transition state TS2′, this structure is in fact obtained

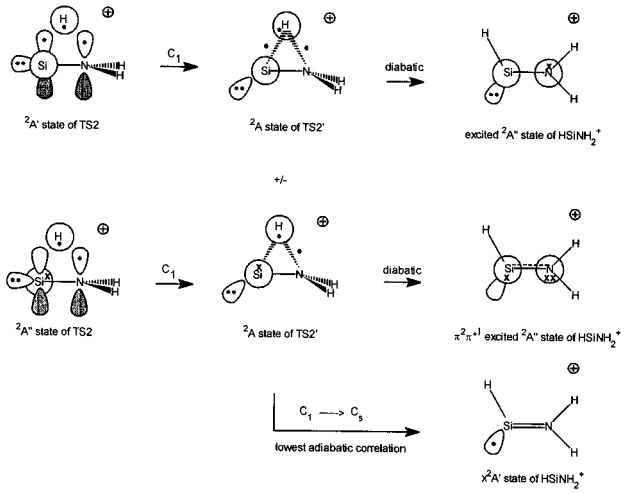

Figure 6. Out-of-plane internal rotation of TS2 toward the planar $HSiNH_2^+$ structure and through TS2′.

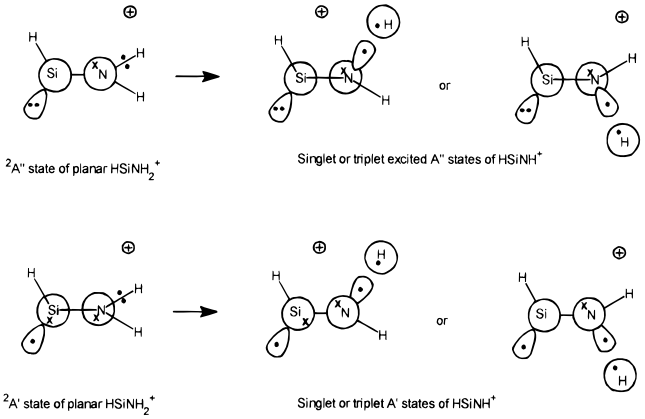

Figure 7. In-plane NH stretch on the planar $HSiNH_2^+$ species.

in its $^2A''$ excited states whatever the initial state of TS2 is (Figure 6): such A″ states cannot adiabatically correlate to the X^2A' ground state of $HSiNH_2^+$. The situation is, however, more subtle; the adiabatic correlation must be made in the transition state symmetry group, namely C_1, so that both the A states of TS2′ can mix. Following the *lowest* A potential energy surface (adiabatic correlation) leads then to the $^2A'$ state of $HSiNH_2^+$, whereas following the next energy surface leads either to a A′ or to a A″ state of the planar molecule. The exact symmetry of this second state is, however, of no importance as will be seen below. Despite convergence troubles, which are very certainly due to the flatness of the potential energy surface, it has been possible to locate the lowest C_1 state of TS2′ and to evaluate its vibrational wavenumbers: the imaginary mode at 1466i cm^{-1} corresponds to the out-of-plane rotation towards the planar structure with a strong coupling with other modes such as the in-plane rotation and the stretching of the SiH, NH, and SiN bonds.

The X^2A' ground state of the planar $HSiNH_2^+$ structure has no imaginary frequency as seen from Table 6. From its $^2A''$ state, the in-plane stretch of a NH bond gives a singlet or a triplet state of $HSiNH^+$ having A″ symmetry (Figure 7):

$$KK \,||\, \sigma^2_{SiN}\, sp^2_{Si}\, \sigma^2_{SiH}\, \sigma^2_{NH}\, sp^1_{N}\, \pi^1_{SiN} \qquad (19)$$

Such a configuration corresponds to excited states of $HSiNH^+$ (part I of this series): the corresponding exit channels are thermodynamically closed. At variance, the X^2A' ground state of $HSiNH_2^+$ diabatically undergoes a reaction toward A′ singlet

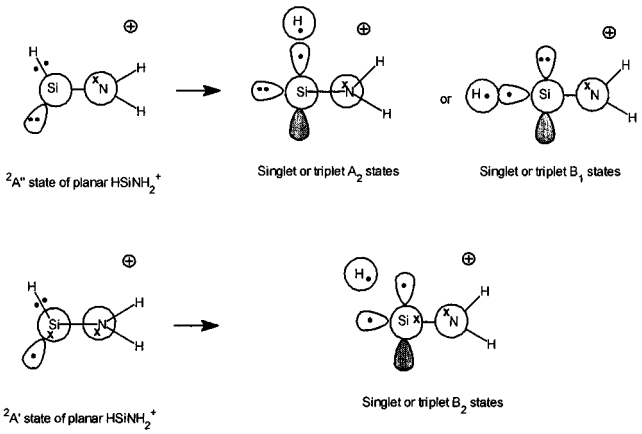

Figure 8. In-plane SiH stretch on the planar $HSiNH_2^+$ species.

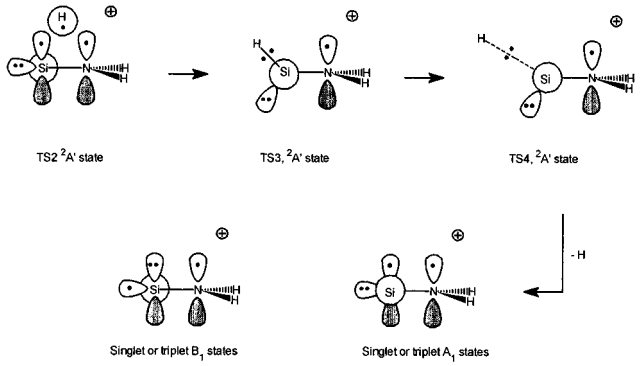

Figure 9. Formation and reaction of TS3 and TS4.

or A′ triplet states of $HSiNH^+$. It follows that the adiabatic correlation of

$$KK \,||\, \sigma^2_{SiN}\, sp^1_{Si}\, \sigma^2_{SiH}\, \sigma^2_{NH}\, sp^1_{N}\, \pi^2_{SiN} \qquad (20)$$

leads to the X^1A' ground state or to the a^3A' state of $HSiNH^+$. The corresponding reactions are

$$Si^+(X^2P) + NH_3 \rightarrow H(^2S) + HSiNH^+(X^1A') \qquad (21)$$

$$Si^+(X^2P) + NH_3 \rightarrow H(^2S) + HSiNH^+(a^3A') \qquad (22)$$

As seen in section 3 and in Table 9, they are endothermic by 34.9 and 79.3 kcal/mol and are thus not possible in interstellar conditions: the question of the possible existence of a barrier along the paths is irrelevant in this case. The same conclusion is all the more valid as the previous correlations are not adiabatic.

Moreover, the in-plane stretch of the SiH bond, even if occuring without barrier, would lead to excited states of $SiNH_2^+$ within the A_2, B_1, or B_2 symmetries as depicted in Figure 8. In that case, the reactions are thermodynamically not possible, as explained in section 4.3.2.

The remaining possibility is to go on rotating the hydrogen on the $^2A'$ state of TS2, ensuring the conservation of the initial symmetry plane. So doing, TS3 is obtained (Figure 5) for which the imaginary frequency (888i cm^{-1}, A″ symmetry) corresponds to the out-of-plane deformation leading to the previous planar $HSiNH_2^+$ species. Once TS3 has been formed, turning the reaction coordinate from the ∠NSiH valence angle to the SiH stretching mode leads to the final transition structure TS4 (Figure 9), where r_{SiH} (2.40 Å) is by far longer than that observed in TS2, TS3, and the planar $HSiNH_2^+$ structure (Tables 4 and 5). The imaginary frequency associated with TS4 (476i cm^{-1}, A′ symmetry) tends to finally break the SiH bond which diabati-

cally gives $SiNH_2^+$ either as $^{1,3}B_1$ states or as $^{1,3}A_1$ states. The adiabatic X^1A_1 exit channel is solely allowed.

Hence, starting from the proper electronic state of the reactants, the previous mechanism (path B) proceeds without activation barrier and is likely to occur in interstellar conditions.

4.5. Sketching Some Dynamical Aspects of the $Si^+ + NH_3$ Reaction. A complete study of the dynamics of the $Si^+ + NH_3$ reaction is beyond the scope of this work. Some important conclusions can, however, be derived from the final potential energy surface presented in Figure 3. First of all, the formation of the long-range $SiNH_3^+$ complex is exothermic, by more than 52 kcal/mol; this is about twice as small as the corresponding value for the $C^+ + NH_3$ reaction.[12] We will make the assumption that the centrifugal barrier occuring on the complexation path can be crossed over thanks to a sufficient collision energy (see below). At variance with $C^+ + NH_3$ for which the first transition state (analogous to TS1 on path A) lies 69.2 kcal/mol below the reactants, this difference is reduced to only 2.5 kcal/mol (corrected MP4 level of calculation, section 4.3.1 and Table 10) for the system being investigated here. Even if an overestimated value of 0.02 eV (0.46 kcal/mol) is assumed for the centrifugal barrier corresponding to the dissociation of TS1 into H and $SiNH_2^+$, reaction path A will have no dynamic barrier as is the case for the latter reaction. Moreover, if path A were the only path opened toward the final products, the very small difference between the energy of the reactants and that of TS1, about 1000 cm^{-1} (2.5 kcal/mol), would imply that the release of only one or two vibrational quanta from the vibrationally excited $SiNH_3^+$ complex makes this species either driven back to the reactants or possibly stabilized in the well. It is then likely that it could tunnel toward the planar $HSiNH_2^+$ structure, since its energy is slightly lower. Flores et al.[36] have proposed the first explanation why for this reaction

$$f = k_{bim}^{exp}/k_c^{exp} \approx 1/3 \qquad (23)$$

where k_{bim} is the bimolecular rate coefficient (*i.e.*, the rate the long-range complex disappears toward the products) and k_c is the capture rate coefficient (*i.e.*, the rate the long-range complex is formed from the reactants). Although we do not perform any rate coefficient determination in the present paper, the knowledge of detailed correlation diagrams and accurate energetic values allow to perform a refined analysis of this experimental observation.

Why *f* differs from unity comes primarily from the fact that one of the potential surfaces arising from the X^2P state of Si^+ is in fact repulsive (section 4.2, Figure 2, and configuration 12); thus, *f* should be 2/3 since the two remaining lowest $^2A'$ and $^2A''$ surfaces are attractive and lead to $SiNH_3^+$ in its X^2E ground state. However, only one of the components of this state (namely the lowest $^2A'$ substate) correlates to the ground states of the products along path A (section 4.3.1 and Figure 4) and gives an exothermic reaction; the other component correlates to an excited state of $SiNH_2^+$ (section 4.3.2) and gives endothermic reactions. It follows that *only one* potential surface arising from the threefold degenerate ^2P reactive atomic state gives a thermodynamically allowed reaction: *f* ultimately equals 1/3 for path A. A final argument might be given by the calculation of the excited $^2A''$ state of TS1: ref 36 reports that it lies 8.4 kcal/mol above the reactants and concludes to the existence of a barrier along path A-$^2A''$ so that f_A becomes 1/3 instead of 2/3. However, the level of calculation used to locate this excited transition state is questionable. In order to get a better estimate of this energy splitting, MC/P calculations were performed to more accurately locate the excited $^2A''$ state, assuming the geometry of the lowest $^2A'$ state of TS1; so doing, a value of 3.1 kcal/mol is found, relative to the lowest $^2A'$ state. It follows thus that the reactants and TS1-$^2A''$ are at the same energy within 0.5 kcal/mol. As a consequence, the most reliable explanation why f_A equals 1/3 should be seen as the symmetry considerations that rule out path A-$^2A''$ owing to the highly endothermic character of the associated exit channels.

Let us now turn to path B. The highest transition state along path B, namely TS2, lies much more below the reactants (12.5 kcal/mol) than TS1 (2.5 kcal/mol). No barrier occurs, neither thermodynamic nor dynamic, along the path toward TS4, the last stationary point on the surface, *i.e.*, that which undergoes the final SiH stretching dissociation. TS4 lies 20.3 kcal/mol below the reactants: a centrifugal barrier of about 0.02 eV will not bring any dynamic barrier to the final bond breaking. As for path A, two states of TS2 can be obtained from the X^2E state of $SiNH_3^+$. TS2-$^2A'$ clearly lies below TS1-$^2A'$ and can thus be reached with no activation energy from the reactants. Whatever the TS2-$^2A''$ state ultimately correlates to as final products, they are unlikely to be reached in the absence of external energy: using the geometry of the TS2-$^2A'$ state, MC/P calculations reveal that it lies 16.3 kcal/mol *above* the reactants. So that we finally get: $f_B = 1/3$.

From $f_A = 1/3$, and $f_B = 1/3$, we deduce that $f = 1/3$ for the whole reaction. Due to the high location of the transition state along path A, it can be suspected that reaction path B may be more efficient than path A (*i.e.*, has a larger reaction rate) to drive the reactants towards the products.

5. The $N + SiH_3^+$ and $N^+ + SiH_3$ Reactions

Some other reaction schemes have been assumed to be of interest for the HNSi/HSiN system in the ISM.[4] They involve either the reaction of the silyl radical SiH_3 onto N_{II} (reaction 8) or the formation of a complex between N_I and the silyl cation SiH_3^+ (reaction 7).

5.1. $N(X^4S) + SiH_3^+(X^1A_1)$. In that case, and according to the spin conservation laws, a quartet potential energy surface has to be investigated, leading to the consideration of triplet species of $(H, H, Si, N)^+$ stoichiometry in the exit channels. Quintet states are much higher in energy and will not be discussed further. As seen from Table 2, the lowest triplet state on the $(H, H, Si, N)^+$ surface is found to be the planar *cis*-bent triplet state of $HSiNH^+$ (a^3A'). However, as seen from Table 11, the exit channels

$$N(X^4S) + SiH_3^+ \rightarrow H(X^2S) + HSiNH^+(a^3A') \qquad (24)$$

$$N(X^4S) + SiH_3^+ \rightarrow H(X^2S) + SiNH_2^+(1^3B_2) \qquad (25)$$

$$N(X^4S) + SiH_3^+ \rightarrow H(X^2S) + H2SiN^+(X^3A_2) \qquad (26)$$

$$N(X^4S) + SiH_3^+ \rightarrow H(X^2S) + H2SiN^+(1^5B_2) \qquad (27)$$

all are endothermic (or exothermic but spin-forbidden); hence they are not possible in interstellar conditions. Moreover, the $NSiH_3^+(C_{3v})$ complex that would be primarily produced would have a three open-shell configuration:

$$KK \mid\mid \sigma_{SiN}^{\uparrow} 2p_N^{\uparrow} 2p_N^{\uparrow} \qquad (28)$$

Configuration 28 certainly corresponds to a very high energy lying state of the intermediate (quartet state), or even to a repulsive surface: this makes the reaction very improbable (Figure 10a) since a high barrier may exist for the formation of the $NSiH_3^+$ long-range precursor.

TABLE 11: Exothermicity (kcal/mol) for Reactions Investigated in section 5[a]

	$SiNH_2^+$		H_2SiN^+				$HSiNH^+$	
states	X^1A_1	1^3B_2	X^3A_2	1^1A_1	1^3B_2	1^5B_2	X^1A'	a^3A'
relative energies	000	3.68	000	0.86	0.54	4.20	000	1.97
$Si^+(X^2P) + NH_3(X^1A_1)$	−17.4	67.4	106.3	126.1	118.7	(203.1)	34.8	80.1
$N(X^4S) + SiH_3^+(X^1A_1)$	(−83.1)	1.7	40.6	60.4	53.0	137.4	(−30.9)	14.4
$N(a^2D) + SiH_3^+(X^1A_1)$	−138.0	−53.2	−14.3	5.5	−1.87	(82.5)	−85.8	−40.5
$N(b^2P) + SiH_3^+(X^1A_1)$	−165.4	−80.6	−41.7	−21.9	−29.3	(55.1)	−113.2	−67.9
$N^+(X^3P) + SiH_3(X^2A_1)$	−236.9	−152.2	−113.2	−93.5	−42.3	(−16.5)	−184.8	−139.5

[a] Excited states are relative to the ground state for each species (eV). The calculated values have been obtained at MP2/6-311++G** level of theory. C_{3v} and D_{3h} energies and geometries for $SiH_3(X^2A_1)$ and $SiH_3^+(X^1A'_1)$ are respectively $r_{SiH} = 1.473$ Å, apex = 107.7° (−290.852 811 au) and $r_{SiH} = 1.459$ Å (−290.589 813 au). This gives a 7.2 eV adiabatic ionization potential for SiH_3. Vertical excited states of $SiNH_2^+$, H_2SiN^+ have been determined using the MC/P methodology. The excited states of the nitrogen atom and its first ionization potential come from Bacher and Goudsmit:[41] X^4S, 0.00; a^2D, 2.381; b^2P, 3.572; and X^3P, 14.48 eV. Bracketed values indicate spin-forbidden exit channels.

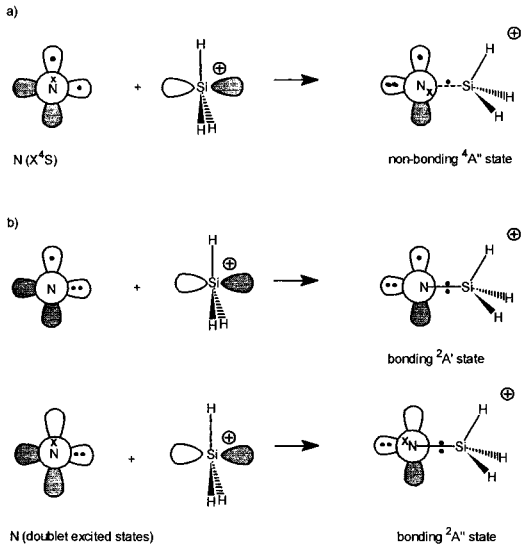

Figure 10. Action of N (X^4S, or excited $2p^2$ doublet states) onto SiH_3^+ ($X^1A'_1$).

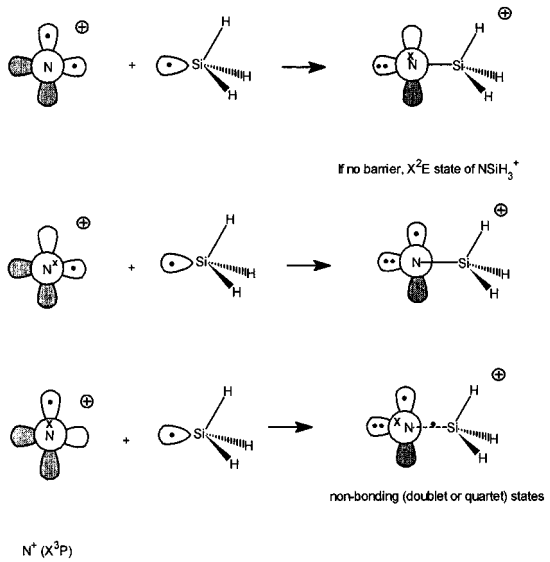

Figure 11. Action of $N^+(X^3P)$ onto $SiH_3(X^2A_1)$.

5.2. $N(a^2D,b^2P) + SiH_3^+(X^1A'_1)$. The only possibility to remain on a doublet surface in order to correlate to the lowest singlet or triplet (Si, N, H, H)$^+$ exit potential energy surfaces is to invoke an excited state of one of the reactants. Excited SiH_3^+ molecules can first be considered, but owing to the low abundance of the yet-undetected neutral precursor, the low abundance of the SiH_3^+ cation, and the even lower abundance of its excited states, this mechanism can be anticipated to be of poor efficiency. Moreover, even the existence of reachable excited states of SiH_3^+ is questionable: valence excited states would correspond either to a $\sigma_{SiH} \rightarrow 3p_{Si}$ or to a $\sigma_{SiH} \rightarrow \sigma^*_{SiH}$ excitation. In both cases, the corresponding states are likely to dissociate to H^+ and SiH_2. Excited states of N_I appear thus as more attractive candidates in ISM conditions.

Let us first consider the a^2D state lying at 2.381 eV above the X^4S ground state.[41] The long-range $NSiH_3^+$ complex might form (Figure 10b), in a ^2E state (with $^2A'$ and $^2A''$ components), at least from some components of the atomic state. Then, following the possible evolutions discussed in section 4, the dissociation obtained through a SiH bond stretch can be hypothetized: this gives H_2SiN^+, singlet or triplet, as the exit channels. As seen in Table 11, the triplet exit channel is open whereas the singlet one is not. A second path is obtained through the transfer of an hydrogen atom toward the nitrogen atom in order to get H_2SiNH^+. In that case, the dissociative stretch of the NH bond still leads to H_2SiN^+, singlet or triplet. Stretching a SiH bond leads, however, to $HSiNH^+$ and to a strongly exothermic reaction (Table 11). Finally, if we make the assumption that one more hydrogen can rotate from Si toward N, $HSiNH_2^+$ is obtained and can evolve without barrier to $SiNH_2^+$ as explained in section 4. A symmetry analysis such as that given in section 4 would be possible in order to check if reactants adiabatically give the products corresponding to thermodynamically-open exit channels. The experience on the previous $Si^+(X^2P) + NH_3$ reaction has shown, however, that all spatial symmetries were allowed as exit channels, either as singlet or triplet spin states, provided the right component of the initial atomic state was considered. There is thus no reason why the situation should be different here.

If we now turn to the b^2P state of the nitrogen atom, 3.572 eV above the ground state, exactly the same conclusions can be derived, with the noticeable exception that much more exit channels are allowed now (Table 11). Hence, only the existence of activation barriers would have the corresponding reactions impeached in interstellar conditions. Are all these reactions finally relevant in the ISM? Certainly not in dark clouds where the abundance of excited N_I is almost negligible.

5.3. $N^+(X^3P) + SiH_3(X^2A_1)$. There is no doubt that the abundance of N_{II} is extremely low in molecular clouds: owing to the lack of UV radiations and the low temperature, it seems unlikely that the ionization of N_I, which requests 14.48 eV, is efficient. As a consequence, the low abundance of the reactants makes the running reaction rather exotic and certainly not a dominant process. Nevertheless, one of the three components of the X^3P (uncoupled $2p^2$ configuration) ground state of N+ is likely to give a poorly attractive, and even a repulsive, surface upon complexation with $SiH_3(X^2A_1)$ (Figure 11), whereas the two other components might give a ^2E state of the complex. Whether this complexation occurs with a barrier or not cannot be derived from simple correlation diagrams. The thermody-

namics is favorable (Table 11), however. A different situation prevails for the $2p^2$ excited states of N_{II} since only $\sigma^1_{NSi}\, 2p^2_N$ and $\sigma^2_{NSi}\, \sigma^{*1}_{NSi}$ molecular states would be obtained in those cases, which leads either to a high excited state of the complex, or even to repulsive surfaces.

6. Further Evolutions of $SiNH_2^+$

As anticipated previously, once $SiNH_2^+$ has been formed it is likely to undergo dissociative recombinations which are presently under investigations. Three different schemes have to be considered:

$$SiNH_2^+ + e^- \rightarrow HNSi + H \quad (29)$$

$$SiNH_2^+ + e^- \rightarrow SiN + H_2 \quad (30)$$

$$SiNH_2^+ + e^- \rightarrow Si + NH_2 \quad (31)$$

They either break the SiN bond or lead to HNSi or to SiN, which thus appear as the only possible azasilicated products arising from $Si^+ + NH_3$. The nondetection of HNSi may indicate either that the recombination favors the production of SiN or that today's radiodetectors are not sensitive enough to record the spectra of low-abundance species having a dipole moment less than 0.1 D.

If HSiN, the dipole moment of which does not preclude its radio detection in the ISM, is observed, then other reaction schemes than those studied here will have to be proposed to explain its formation. One possibility would be that the $SiNH_2$ neutral species, which is the intermediate in the previous recombinations, could rearrange to neutral H_2SiN or HSiNH: such processes are very improbable since preliminary investigations show that $SiNH_2$ is the absolute minimum of the neutral (H, H, Si, N) potential energy surface. Finally, reactions 32 and 33

$$HNSi^+ + e^- \rightarrow SiN + H \quad (32)$$

$$HSiN^+ + e^- \rightarrow SiN + H \quad (33)$$

that would explain the existence of SiN and the lack of both the HSiN and HNSi species as a consequence of the dissociative recombinations on their cations certainly do not take place efficiently in interstellar clouds: the adiabatic ionization potentials of HNSi and HSiN to the corresponding $X^2\Sigma^+$ cations are estimated to be as high as 11.4 and 11.9 eV at the MP2/6-311++G** level of theory.

7. The HSiN + H^+ ↔ HNSi + H^+ Reactions. Can HSiN Finally Survive Interstellar Conditions?

At the end of this report, the question remains whether there exists a reaction leading efficiently to HSiN in interstellar conditions or not. Another approach to assess the feasibility of detecting HSiN in the ISM should not consider the ways HSiN can be produced but the ways it can be destroyed: whether HSiN, once formed, can survive in molecular clouds or not is certainly the most crucial problem. Within this viewpoint, the following reactions have to be investigated:

$$HSiN + H \rightarrow HNSi + H \quad (34)$$

$$HSiN + H^+ \rightarrow HNSi + H^+ \quad (35)$$

Both reactions have been investigated at the MP2/6-311++G** level of calculation. The corresponding adiabatic potential energy surfaces are presented in Figure 12 and the related geometries and vibrational wavenumbers in Table 12. It is clearly illustrated that HSiN isomerizes to HNSi without barrier in these addition/elimination processes, whether the reaction involves a neutral hydrogen atom or a naked proton. In the case of reaction 35, the path to $SiNH_2^+$ has been added: the intrinsic barrier for the $HSiNH^+ \rightarrow SiNH_2^+$ rearrangement is 15.6 kcal/mol, so that it can be crossed if starting from HSiN and H^+.

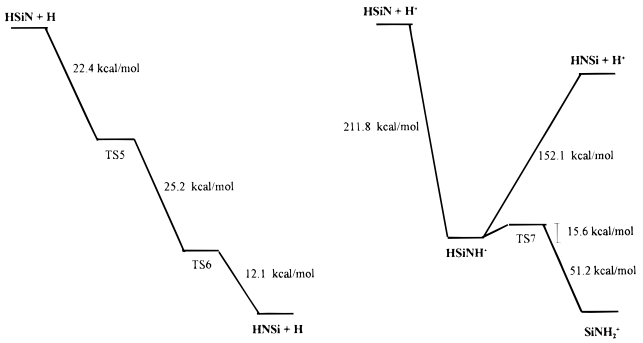

Figure 12. HSiN + H^+ ↔ HNSi + H^+ reactions.

TABLE 12: Energetics, Geometries (Å and deg) and Scaled Vibrational Wavenumbers for the Compounds Involved in Figure 12[a]

	$HSiNH^+$ X^1A' (*trans*)[b]	HSiNH TS5-$^2\Sigma^+$	HSiNH TS6-$^2A'$	$SiNH(H)^+$ TS7-$^2A'$[d]
r_{SiN}	1.536	1.541	1.521	1.572
r_{SiH}	1.457	1.434	1.647	1.543
r_{NH}	1.014	0.997	1.001	1.015
∠HSiN	158.97	180.0	167.5	180.0
∠HNSi	157.59	180.0	178.8	180.0
energy	−344.610561	−344.808280	−344.848496	−344.586319
vibrations[c]	207 A′	904i A′	111i A′	946i A′
	560 A′	201 A′	291 A′	206 A′
	580 A″	672 A″	399 A″	453 A″
	1147 A′	1702 A′	1128 A′	1081 A′
	2174 A′	1721 A′	1726 A′	1659 A′
	3303 A′	2464 A′	3657 A′	3280 A′
		3720 A′		

[a] The 6-311++G** basis set is used. [b] Planar form of the floppy singlet ground state. Dipole moment 2.6 D, B_0 17 500 MHz (see part I of this series). [c] The analysis is performed in C_s symmetry. [d] Quasi-linear structure.

Hydrogenation reactions such as reaction 34 are usually less efficient than protonation processes in dense clouds: however, the situation is rather subtle since the most probable reactant is not a naked proton, but the H_3^+ entity,[42,43] which is among the dominant ions in dense clouds. It follows that the interesting reaction is in fact

$$HSiN + H_3^+ \rightarrow HNSi + H^+ + H_2 \quad (36)$$

Upon formation of ($HSiNH^+\cdots H_2$), the system is likely to release its excess of internal energy as kinetic energy in the two products $HSiNH^+$ and H_2. In that case, the remaining internal energy of $HSiNH^+$ might no longer be sufficient, either to reach the HNSi + H^+ exit channel or even to cross the barrier toward $SiNH_2^+$; if we assume that the tunneling $HSiNH^+ \rightarrow SiNH_2^+$ is poorly efficient due to the height of the barrier (15.6 kcal/mol), then $HSiNH^+$ could be stabilized and could undergo a dissociative recombination toward HSiN or/and HNSi. Thus, the complexation of HSiN with H_3^+ followed by the dissociative recombination of $HSiNH^+$ formally results either in destroying HSiN if the recombination leads to HNSi or in driving the system back to reactants (except that H_3^+ has been dissociated into H_2 and H^+) if the recombination lead to HSiN. At variance, if the tunneling process from $HSiNH^+$ is dominant relative to

the recombination, HSiN is transformed to $SiNH_2^+$. In any case, there will be no accumulation of HSiN in the ISM if only the previous mechanisms are considered.

The leading conclusion of this section remains that *HSiN is unlikely to survive hydrogenation processes in interstellar environments*, in contrast to HNSi. If we assume that a very efficient process exists that produces both HSiN and HNSi so that the ratio [HSiN/HNSi] is close to unity in the absence of destruction mechanisms, then the consideration of reactions such as reaction 36 results in having finally [HSiN/HNSi] $\ll 1$. The detection of HSiN, which has a large dipole moment, would mean that an extremely efficient reaction produces HSiN and competes with reactions 9, 29, and 36. The existence of such a process seems to be very questionable.

8. Conclusions

In the present paper, an accurate *ab initio* study of the (Si, N, H, H, H)$^+$ potential energy surface has been reported. Starting from $Si^+(X^2P)$ and $NH_3(X^1A_1)$, this study shows that only the exit channel toward $H(X^2S)$ and $SiNH_2^+(X^1A_1)$ is thermodynamically open. Two different reaction paths have been found that connect the reactants to the products: both proceed without activation barrier and have been thoroughly described using symmetry analysis and correlation diagrams. Other reactions such as $N + SiH_3^+$ and $N^+ + SiH_3$ have been investigated: they are either forbidden or very unlikely to occur in standard interstellar conditions because the reactants are to be in excited states which cannot be efficiently populated.

Contrary to what is known in carbon−nitrogen chemistry where the $HCNH^+$ is the key intermediate, it is the $SiNH_2^+$ species which is the *key entity* when dealing with the interstellar chemistry of silicon and nitrogen. Upon its dissociative recombination, it is anticipated that only SiN or/and the sole HNSi isomer can be formed. Hence, the very low dipole moment of HNSi is certainly the most probable reason why this molecule has not yet been detected in interstellar clouds.

At variance, HSiN, the higher isomer of HNSi has been found to be produced by none of the reactions studied here. Although having a large dipole moment (4.5 D), the lack of detection of this species in the interstellar medium may indicate that, even if formed by some mechanism overlooked in the present report, HSiN might, in fact, be unlikely to survive interstellar conditions as discussed in the final section; upon hydrogenation processes, for example, it isomerizes to HNSi without activation barrier.

Acknowledgment. Part of the calculations presented here were supported by the CNRS Institut du Développement et des Ressources en Informatique Scientifique (IDRIS). This research was also partly conducted with the supercomputer resources at the Jet Propulsion Laboratories (JPL), California Institute of Technology, under contract to the National Aeronautics and Space Administration (NASA).

References and Notes

(1) Turner, B. E. *BAAS* **1991**, *23*, 933.
(2) Turner, B. E. *Astrophys. J.* **1991**, *371*, 573.
(3) Turner, B. E. *Astrophys. J.* **1992**, *388*, L35.
(4) Herbst, E.; Millar, T. J.; Wlodek, S.; Bohme, D. K. *Astron. Astrophys.* **1989**, *222*, 205.
(5) Langer, W. D.; Glassgold, A. E *Astrophys. J.* **1990**, *352*, 123.
(6) Adams, W. *Astrophys. J.* **1941**, *93*, 11.
(7) Green, S.; Herbst, E. *Astrophys. J.* **1979**, *229*, 121.
(8) Ziurys, L. M.; Turner, B. E. *Astrophys. J.* **1986**, *302*, L31.
(9) Scuseria, G. E.; Lee, T. J.; Saykally, R. J.; Schaeffer, H. F. *J. Chem. Phys.* **1986**, *84*, 3703.
(10) Herbst, E. *Astrophys. J.* **1978**, *222*, 508.
(11) Foresman, J. B.; Head-Gordon, M.; Pople, J. A. *J. Phys. Chem.* **1992**, *96*, 135.
(12) Talbi, D.; Ellinger, Y., submitted for publication.
(13) Ogilvie, J. F.; Cradock, S. *Chem. Commun.* **1966**, 364.
(14) Maier, G.; Glatthaar J. *Angew. Chem., Int. Ed. Engl.* **1994**, *33*(4), 473.
(15) Maier, G.; Glatthaar J.; Reisenauer, H. P. *Chem. Ber.* **1989**, *122*, 2403.
(16) Bogey, M.; Demuynck, C.; Destombes, J. L.; Walters, A. *Astron. Astrophys.* **1991**, *244*, L47.
(17) Elhanine, M.; Hanoune, B.; Guelachvili, G. *J. Chem. Phys.* **1993**, *99*(7), 4970.
(18) Parisel, O.; Hanus, M.; Ellinger, Y. *Chem. Phys.*, in press.
(19) Goldsmith P.; Irvine, W.; Hjalmarson, A.; Ellder, J. *Astrophys. J.* **1986**, *310*, 383.
(20) Talbi, D.; Ellinger, Y.; Herbst, E. *Astron. Astrophys.* **1996**, *314* (2), 688.
(21) Parisel, O.; Hanus, M.; Ellinger, Y. *J. Phys. Chem.* **1996**, *100*(8), 2926.
(22) Parisel, O.; Hanus, M.; Ellinger, Y. *J. Chem. Phys.* **1996**, *104*(5), 1979.
(23) Parisel, O.; Ellinger, Y. *Chem. Phys.* **1994**, *189*, 1.
(24) Parisel, O.; Ellinger, Y. *Chem. Phys.* **1996**, *205*, 323.
(25) Clark, T.; Chandrasekhar, J.; Spitznagel, G. W.; Schleyer, P. v. R. *J. Comput. Chem.* **1983**, *4*, 294.
(26) Frisch, M. J.; Pople, J. A.; Binkley, J. S. *J. Chem. Phys.* **1984**, *80*, 3265.
(27) Krishnan, R.; Binkley, J. S.; Seeger, R.; Pople, J. A. *J. Chem. Phys.* **1980**, *72*, 650.
(28) McLean, A. D.; Chandler, G. S. *J. Chem. Phys.* **1980**, *72*, 5639.
(29) *Gaussian 92*, Revision E.1; Frisch, M. J.; Trucks, G. W.; Head-Gordon, M.; Gill, P. M. W.; Wong, M. W.; Foresman, J. B.; Johnson, B. G.; Schlegel, H. B.; Robb, M. A.; Replogle, E. S.; Gomperts, R.; Andres, J. L.; Raghavachari, K.; Binkley, J. S.; Gonzalez, C.; Martin, R. L.; Fox, D. J.; Defrees, D. J.; Baker, J.; Stewart, J. J. P.; Pople, J. A. Gaussian Inc.: Pittsburgh, PA, 1992.
(30) Boys, S. F.; Bernardi, F. *Mol. Phys.* **1970**, *19*, 553.
(31) Hobza, P.; Zahradnik, R. *Chem. Rev.* **1988**, *88*, 871.
(32) Flores, J. P.; Gomez Crespo, F.; Largo-Cabrerizo, J. *Chem. Phys. Lett.* **1988**, *147*(1), 84.
(33) Flores, J. P.; Largo-Cabrerizo, J. *Chem. Phys. Lett.* **1989**, *183*, 17.
(34) Ye, S.; Dai, S. *Chem. Phys. Lett.* **1991**, *236*, 259.
(35) Parisel, O.; Hanus, M.; Ellinger, Y. About the formation of interstellar SiN. In: *Molecules and Grains in Space*; AIP Conference Proceedings 312; Nenner, I., Ed.; AIP Press: New York, 1994; p 515.
(36) Flores, J. P.; Redondo P.; Azpeleta S. *Chem. Phys. Lett.* **1995**, *240*, 193.
(37) Goldberg, N.; Hrusak, J.; Iraqi, M.; Schwarz, H. *J. Phys. Chem.* **1993**, *97*, 10687.
(38) Goldberg, N.; Iraqi, M.; Hrusak, J.; Schwarz, H. *Int. J. Mass Spectrom. Ion Processes* **1993**, *125*, 267.
(39) Wlodek, S.; Rodriquez, C. F.; Lien, M. H.; Hopkinson, A. C.; Bohme, D. K. *Chem. Phys. Lett.* **1988**, *143*(4), 385.
(40) Allen, T. L.; Goddard, J. D.; Schaefer, H. F. *J. Chem. Phys.* **1980**, *73*(7), 3255.
(41) Bacher, R. F.; Goudsmit S. *Atomic Energy States*; McGrawHill: New York, London, 1932.
(42) Watson, W. D. *Rev. Mod. Phys.* **1976**, *48*, 513.
(43) Irvine, W. M.; Goldsmith, P. F.; Hjalmarson, A. In *Interstellar Processes*; Hollenbach, D. J., Thoronsson, H. A., Eds.; Reidel: Dordrecht, 1987; p 561.